Three-Dimensional Strain of a Portion of the Walker Lane Using SIR-B and Geophysical Data

Marcus Borengasser

Abstract

The Walker Lane is a northwest-trending zone about 700 km long and 100 to 300 km wide in the western Great Basin. The odd-axis model of Krantz (1988) was used to model the three-dimensional strain in the Walker Lake and Excelsior-Coaldale sections of the Walker Lane in western Nevada. Earthquake focal mechanisms have a fault/auxiliary plane parallel or subparallel with a SIR-B structural feature. Focal mechanisms indicate strike-slip movement for the Excelsior-Coaldale section, and primarily a dip-slip component for the Walker Lake section. Three-dimensional strain analysis indicates a constricted (prolate) ellipsoid for the Walker Lake section and a flattened (oblate) ellipsoid for the Excelsior-Coaldale section. The differences in the strain ellipsoids are attributed to the fact that regional Walker Lane shear is accommodated independently within the two sections, and not expressed as through-going strike-slip faults. Variations in the three-dimensional strain are also likely to be a result of the rheological anisotropy between the two sections, as well as inherited Mesozoic (?) structures.

Geology of Mineral County

The study area, shown in Figure 1, is in western Nevada and includes eastern Mineral County and parts of Nye and Esmeralda Counties. It measures 45' of latitude by 45' of longitude and has an area of approximately 5427 km^2. Mesozoic granitic rocks outcrop throughout the area and probably underlie most of the ranges; a few outcrops of gabbroic rocks occur in the northwest part of the study area in the Gillis Range. Cambrian, Ordovician, and Devonian rocks are limited to the Candelaria Hills and Miller Mountain area in the southern part of the study area, and Mississippian and Pennsylvanian rocks occur mostly in the central portion in the eastern Excelsior Mountains. Mesozoic sedimentary rocks are present in nearly all the ranges but are most abundant in the Garfield Hills, Gabbs Valley Range, and Gillis Range (north central part of the study area). Small outcrops of allochthonous rocks occur throughout the study area. Extensive Tertiary volcanism has emplaced a variety of volcanic rocks throughout the entire study area (Figure 1).

The highest tectonic units in the study area are the Pamlico and Luning allochthons (Oldow, 1981; Speed, 1978). Each has many nappes containing Mesozoic rocks in which early structures indicate shortening normal to strikes of nappe boundaries and deformation probably contemporaneous with thrusting. The Luning allochthon includes thrust slices of basement of the Triassic shelf carbonates, the main constituents of the allochthon. The basement rocks are the Sonomia arc volcanics, which were probably no deeper than 3 or 4 kilometres at the onset of thrusting. Basement nappes are not recognized in the Pamlico allochthon, perhaps because the Triassic intra-arc or backarc strata it contains were very thick compared to Triassic shelf facies in the Luning allochthon. The maximum age of onset of thrusting in both allochthons is Early Jurassic, and final emplacement of the Luning allochthon was probably Late Cretaceous (Speed and Kistler, 1980).

The Golconda allochthon comprises a succession of nappes of multiply folded and cleaved strata. The nappes dip away from the continent as do early flattening structures. In the Toiyabe Range, east of the study area, Babaie (1984) found that the allochthon has at least 7 kilometres of structural thickness and that virtually all deformation in the allochthon was completed by the time of final emplacement. The Golconda allochthon was transported in a nonmetamorphic environment during the Sonoma orogeny (Saleeby *et al.*, 1986).

Characteristics of the Walker Lane

The Walker Lane (Billingsley and Locke, 1939) is a northwest-trending zone about 700 km long and 100 to 300 km wide in the western Great Basin. It is characterized by strike-slip faults, and by mountain ranges with unusual shapes or trends lying between the Sierra Nevada on the west and areas of long north-northwest-trending mountains and valleys typical of basin-range topography on the east (Stewart, 1988). Stewart (1988) proposed that the zone was initiated in the Mesozoic, and that Mesozoic structures were reactivated and new structures were developed in the Cenozoic. He emphasized the importance of the geology of the Walker Lane in understanding the Mesozoic and Cenozoic history of the western U.S., in addition to revealing the style of Cenozoic strike-slip deformation in a region well inland from the present transform plate boundary.

Stewart (1988) subdivided the Walker Lane into nine structural blocks or sections, each of which generally acted independently of adjacent blocks. All of these blocks contain or are bounded by strike-slip faults, although faults in any one block rarely extend into an adjacent block (Stewart, 1988).

Walker Lake Section

The Walker Lake section contains prominent subparallel north-northwest-trending faults, some of which are considered to be right-lateral faults and others basin-range normal

Spectro Scan, Inc., 190 Rocket Lane #92, West Melbourne, FL 32904.

Photogrammetric Engineering & Remote Sensing, Vol. 61, No. 6, June 1995, pp. 721–729.

0099-1112/95/6106–721$3.00/0

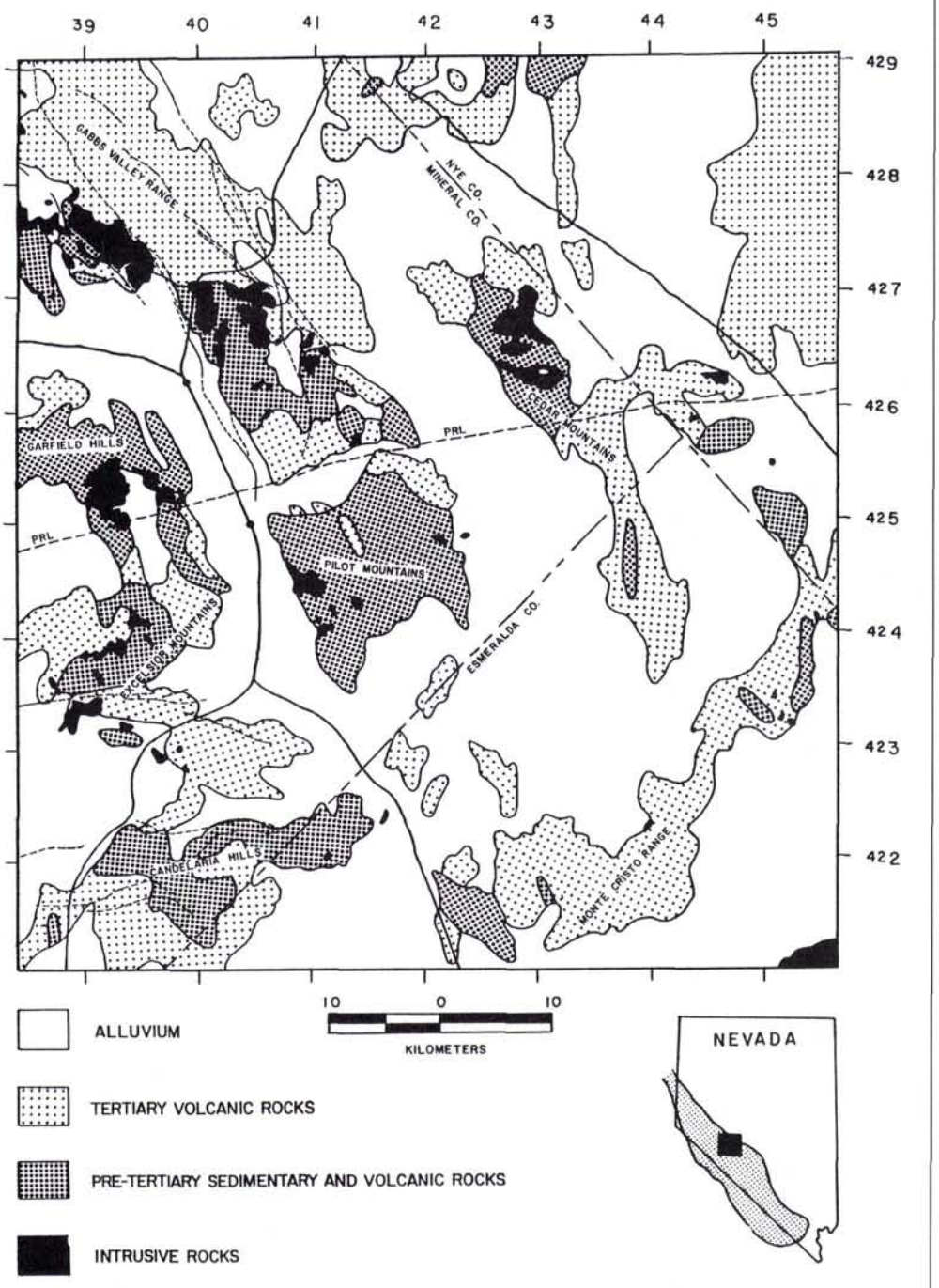

Figure 1. Generalized geologic map of the study area. Inset map shows the location of the study area and the Walker Lane (stippled).

faults. The trends of these faults are at an angle of about 40° to typical north-northeast-trending basin-range faults east of the Walker Lane (Stewart, 1988).

Basin-range normal faults in the Walker Lake section have irregular map traces and bound major west-tilted mountain blocks. On one of the faults on the western margin of the Gabbs Valley Range (Figure 1), striae have rakes of about 60° and plunge to the south, where the fault strike is about N20°W and the dip is 45° east (R. C. Bucknam *in* Zoback, 1986). These basin-range faults are subparallel to right-slip faults to the east (Ekren *et al.*, 1980; Ferguson and Muller, 1949; Nielsen, 1965) that are characterized by generally straight map traces, little topographic relief across them, steep fault planes, and low-angle to horizontal striae on fault

surfaces (Ekren and Byers, 1984; Hardyman, 1978, 1984). Displacements on these right-slip faults have been estimated from the apparent offset of the outcrop limits of Oligocene tuffs that suggest from a few kilometres to as much as 18 kilometres of offset on individual faults, and 48 to 60 kilometres of cumulative offset across the entire fault zone (Ekren and Byers, 1984; Ekren *et al.*, 1980; Hardyman, 1984; Hardyman *et al.*, 1975).

The overlap of landslide deposits considered to be related to strike-slip movement by 24 m.y.-old tuffs, and the deposition of a 22 to 24 m.y.-old tuff against a preexisting fault surface, has been cited as evidence (Ekren and Byers, 1984) that movement on strike-slip faults in the Walker Lake section commenced about 24 m.y. ago (Stewart, 1988). Offset of younger Tertiary rocks and of Quaternary alluvial deposits indicates that normal to strike-slip displacement has continued into the Holocene (Stewart, 1988). Surface rupture occurred in the southern part of the Walker Lake section, a short distance east of the southern part of Petrified Spring-Bettles Well fault, during the 7.2- to 7.3-magnitude Cedar Mountain earthquake of 1932 (Gianella and Callaghan, 1934; Molinari, 1984). Surface faulting was right-normal oblique slip and occurred along a system of generally north-northwest-trending faults (Stewart, 1980).

Excelsior-Coaldale Section

The Excelsior-Coaldale section is a structurally important zone of east-west-trending faults cutting across the dominant north-northwest grain of the Walker Lane Belt (Carr, 1984; Stewart, 1988). The faults appear to have had major right slip in the Mesozoic and local slip in the Cenozoic (Stewart, 1988). This section involves a change, or disruption, in the trends of Precambrian, Paleozoic, and Mesozoic thicknesses, facies, and structural features. These trends are generally south-southwest in central Nevada, but in the Excelsior-Coaldale section are either offset right-laterally (Stewart, 1988) or curve sharply westward (Albers, 1967, Oldow, 1984). Farther west, in eastern California, these features trend generally south-southwest (Stewart, 1988).

Right-lateral offset on the Excelsior and Coaldale fault zones appears to be late Mesozoic in age, because the Lower Jurassic Cretaceous (?) Dunlap Formation appears to be offset and mid Cretaceous and younger plutons appear to intrude the faults (Stewart, 1985). The faults locally cut Cenozoic rocks, but lateral displacements, if any, are small compared to Mesozoic displacements. Oligocene and Miocene tuff units may have been displaced 20 to 25 kilometres left-laterally (Stewart, 1985) along the Coaldale fault zones, indicating a reversal in the sense of movement from Mesozoic to Cenozoic. Speed and Cogbill (1979) also indicated a component of left-lateral offset occurred on the Cenozoic Candelaria fault zone that lies between and subparallel to the Excelsior and Coaldale fault zones, and a component of left-lateral movement was also reported on surface ruptures near the Excelsior fault zone during the 6.3-magnitude Excelsior Mountains earthquake in 1934 (Callaghan and Gianella, 1935).

The trend of the Excelsior and Coaldale fault zones is unique for a system of its size in the Walker Lane Belt, and the fault zones truncate other faults in the Walker Lane belt. A major system of northwest-trending normal and right-lateral faults in the Walker Lake section terminates southward at the Excelsior fault zone. The northwest-trending Owens Valley-White Mountain fault system in eastern California, and the Furnace Creek fault zone in eastern California and western Nevada, terminate northward at the Coaldale fault

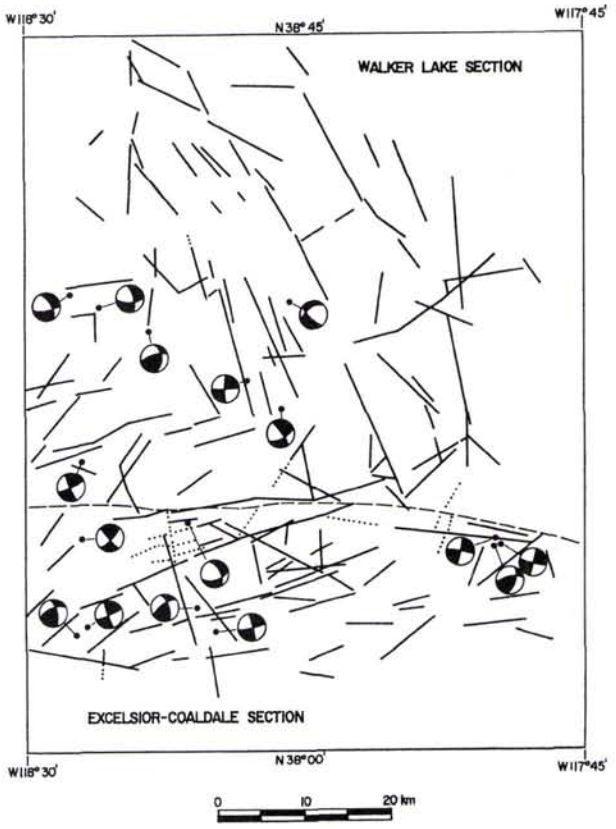

Figure 2. SAR structural features and focal mechanisms for earthquakes used to obtain dip magnitude and dip direction.

zone. This configuration is difficult to relate to the proposed Mesozoic age of the Excelsior and Coaldale faults, and the late Cenozoic age of the northwest-trending faults that they terminate (Stewart, 1988). Stewart (1988) suggested that the northwest-trending faults had a long history and were initiated in the Mesozoic, prior to the Excelsior and Coaldale faults, and were reactivated as major faults in the late Cenozoic. He noted that, if the northwest-trending faults did initiate prior to the Excelsior and Coaldale faults, the curvature of some of the northwest-trending faults, in the vicinity of the Excelsior and Coaldale faults, can be explained as right-lateral drag. Stewart (1988) pointed out, alternatively, that, if displacement on the northwest-trending faults is entirely younger than the Excelsior and Coaldale fault zones, the northwest-trending faults may have terminated against the cross structures of the Excelsior and Coaldale block.

Lineament Characteristics

Figure 2 shows lineaments identified visually from imaging radar data as well as visible/near-IR data sets. Most of the lineaments were mapped from Shuttle Imaging Radar-B (SIR-B) data (October, 1984), and some of them are also visible on the Landsat TM and SPOT panchromatic images. As mentioned above, the study area includes the Walker Lake and Excelsior-Coaldale sections of the Walker Lane. The Walker Lake section is characterized by northwest-trending faults

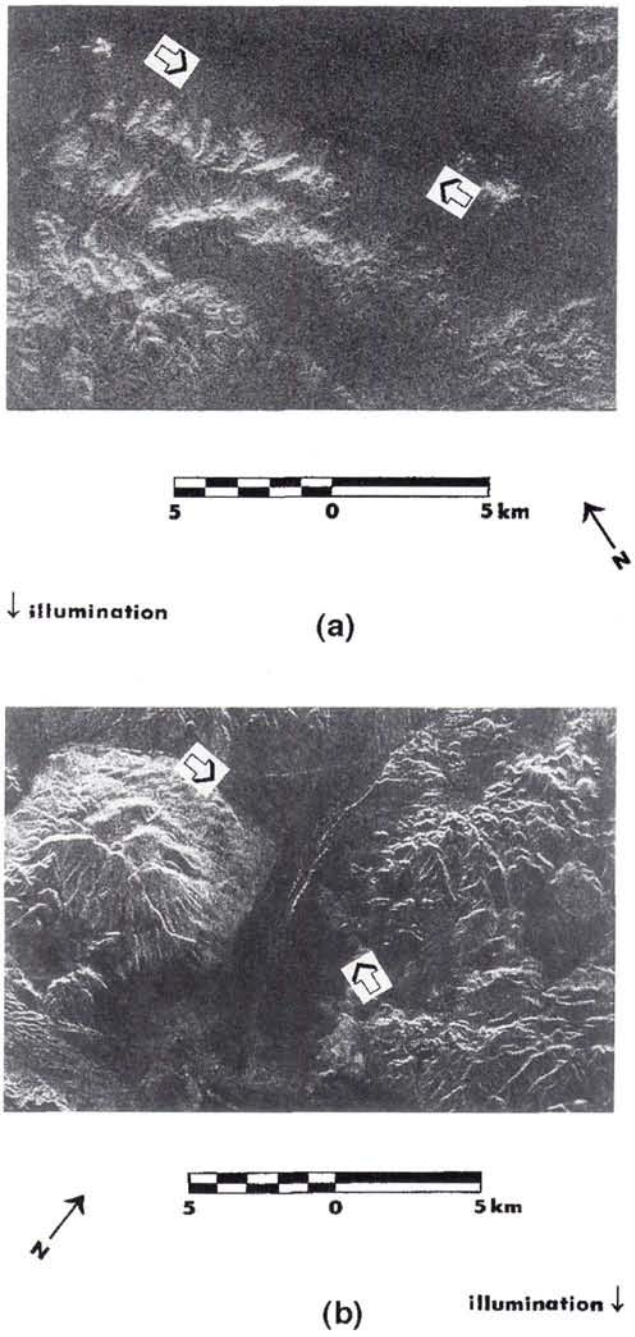

Figure 3. (a) SIR-B Data Take AL55.4, Scene 14, showing northwest-trending structural feature within the Walker Lake section of the Walker Lane. Bright areas are the towns of Luning (north) and Mina (south). (b) SIR-B Data Take AM82.2, Scene 5, showing an east-northeast-trending structural feature within the Excelsior-Coaldale section of the Walker Lane.

and the Excelsior-Coaldale section is characterized by east-northeast trending faults. Lineaments mapped from the remote sensing data sets are very similar in trend to these two fault sets. In addition to the lineaments that coincide with faults in these sections, there are also a large number of lineaments that are parallel to the faults. Of particular interest is the observation that many lineaments that are parallel to the Excelsior-Coaldale set occur in the Walker Lake section and that lineaments parallel to the Walker Lake set occur within the Excelsior-Coaldale section. This suggests that the boundary between the two sections, the Excelsior-Coaldale fault (Stewart, 1988), is not a modern boundary, although it may have been a modern boundary in the past.

The character of synthetic aperture radar (SAR) data is mainly a function of surface roughness, surface geometry, and the complex dielectric constant of rocks and soil. For delineating faults, the SAR signal would respond to a contrast in surface roughness resulting from either additional erosion of a slightly elevated surface or a change in vegetation type or density. A fault can also cause a change in permeability for ground water movement that would result in contrasting soil moisture, or complex dielectric constants, on either side of the fault. Faults that can be detected from these phenomena would generally be located in unconsolidated alluvial material.

By comparison, faults in bedrock can be of any age. Faults in bedrock that are expressed as a topographic feature or by the juxtaposition of lithologies with contrasting roughness can usually be delineated by SAR systems. Considering these factors, good agreement can be expected between location and azimuth of mapped faults and SAR structural features, although mapped faults will often be shorter in length. In unconsolidated materials there are typically few mapped faults, but potentially many SAR structural features. Mapped faults in bedrock coincide with SAR structural features in many cases, such as the Garfield Hills, while areas with unconsolidated materials are dominated by SAR structural features that typically trend parallel to a regional fault set.

Structural features in unconsolidated or alluvial materials are easily delineated with SAR data. Among the many structural features shown on Figure 2, several from the northwest-trending set and the east-northeast-trending set traverse alluviated areas. A northwest-trending feature is located between Luning and Mina, just west of Highway 95. On SIR-B Data Take AL55.4, Scene 14, this feature appears as a distinct line separating areas of contrasting signal return; the western side has the higher signal return (Figure 3a). An east-northeast-trending feature is located on the south end of Teels Marsh. On SIR-B Data Take AM82.2, Scene 5, this feature also appears as a distinct line separating areas of contrasting signal return (Figure 3b). In this case, however, the western half of the structural feature has a higher signal return on the south side, and for the eastern half it is higher on the north side.

Three-Dimensional Strain

Krantz (1988) described a model for the determination of three-dimensional strain from fault data, known as the odd-axis model. The odd-axis model determines the orientation of the principal strain axes (E_x, E_y, E_z, where $E_x > E_y > E_z$) and their relative magnitudes from orientations of fault planes and slip vectors. Only the strain accommodated by slip along the faults is considered. The model assumes that the strain is irrotational, an assumption that seems valid for the study area, because most of the SAR structural features are in Holocene or younger sediments and it is very unlikely that rotation has occurred in that brief period. The model

also assumes that slip is equally distributed among the fault sets and the individual faults.

The foundation of the odd-axis model is the recognition of the "odd" axis: the one principal strain axis with sign opposite the other two, assuming a three-dimensional, constant volume strain field. If one principal extension (strain) is positive and the other two are negative, then the E_x axis is the odd axis. If one principal extension is negative and the other two are positive, then the E_z axis is the odd axis. The intermediate axis (int), E_y, and the similar axis (sim) share the same sign. The similar axis must be E_z where the odd axis is E_x, and vice versa (Krantz, 1988).

Krantz (1988) developed equations to calculate the strain in the principal directions. These equations, listed below, require a value for the final extension length (l'), as well as α, the angle between the intermediate axis and the strike of the fault (set) as measured in the intermediate-similar plane, δ, the dip of the fault measured from the intermediate-similar plane, and the ratio of fault slip to fault spacing (R).

$$E_{int} = \frac{(l'_{int}\, R/2)\sin^2\alpha \sin 2\delta}{l'_{int} - (l'_{int}\, R/2)\sin^2\alpha \sin 2\delta} = \frac{(R/2)\sin^2\alpha \sin 2\delta}{1 - (R/2)\sin^2\alpha \sin 2\delta} \quad (1)$$

$$E_{sim} = \frac{(l'_{sim}\, R/2)\cos^2\alpha \sin 2\delta}{l'_{sim} - (l'_{sim}\, R/2)\cos^2\alpha \sin 2\delta} = \frac{(R/2)\cos^2\alpha \sin 2\delta}{1 - (R/2)\cos^2\alpha \sin 2\delta} \quad (2)$$

$$E_{odd} = \frac{-(l'_{odd}\, R/2)\sin 2\delta}{l'_{odd} - (l'_{odd}\, R/2)\sin 2\delta} = \frac{-(R/2)\sin 2\delta}{1 - (R/2)\sin 2\delta} \quad (3)$$

For strain ratios, however, the final extension length (l') is factored out, and the ratios are functions of fault strike and dip, and the ratio of fault slip to fault spacing: i.e.,

$$E_{int}/E_{sim} = \tan^2\alpha \frac{(1 - (R/2)\cos^2\alpha \sin 2\delta)}{(1 - (R/2)\sin^2\alpha \sin 2\delta)} \quad (4)$$

$$E_{int}/E_{odd} = -\sin^2\alpha \frac{(1 - (R/2)\sin 2\delta)}{(1 - (R/2)\sin^2\alpha \sin 2\delta)} \quad (5)$$

$$E_{sim}/E_{odd} = -\cos^2\alpha \frac{(1 - (R/2)\sin 2\delta)}{(1 - (R/2)\cos^2\alpha \sin 2\delta)} \quad (6)$$

These equations express the ratios of principal extensions as functions of fault strike and dip (as measured with the odd axis vertical) and the ratio of fault slip to fault spacing. These equations describe ratios of strain, and the number of fault sets involved is immaterial (Krantz, 1988). Krantz (1988) derived the equations without restrictions on the magnitude of fault slip, so they are valid for both finite and infinitesimal strains. The critical parameter is not the magnitude of strain but the ratio of average fault slip to average fault spacing (Krantz, 1988).

For fault systems where the ratio of fault slip to fault spacing is small, the equations for strain can be greatly simplified. As the ratio of fault slip to fault spacing (R) approaches zero, the fractional term in each of the strain ratio equations (Equations 4, 5, and 6) approaches unity, so that

$$E_{int}/E_{sim} = \tan^2\alpha \quad (7)$$

$$E_{int}/E_{odd} = -\sin^2\alpha \quad (8)$$

$$E_{sim}/E_{odd} = -\cos^2\alpha \quad (9)$$

Alpha, the angle between the intermediate axis and the strike of the fault set as measured in the intermediate-similar plane, is the orientation of the plane representing the fault set relative to the principal strain axes (Krantz, 1988).

Applying the Odd-Axis Model

The mean direction of poles to planes of fault sets can be used for the odd-axis construction. Because the odd axis lies in the intersection of the planes defined by the poles to the faults, a simple stereonet construction can be used to solve for the odd axis. The construction begins by plotting the poles to the faults on a stereonet. The mean of each set of poles is determined. Slip directions for the faults are also plotted. The stereonet is oriented so that the mean poles to two fault sets, and their slip directions, coincide with a great circle. The great circles connecting the mean poles and slip directions of each fault set intersect to form a line, and this line is the odd-axis. The similar and intermediate axes are located on the plane perpendicular to the odd axis. The similar axis, which will be either the E_z or the E_x axis, will bisect the acute angle between the great circles. The intermediate axis will bisect the obtuse angle, 90° from both the odd and similar axes. After defining the orientation of the odd axis, whether it is the E_z or E_x axis can be determined on the basis of additional structural geological information. Fault systems with extension in the odd axis direction imply that E_x is the odd axis; shortening in the odd-axis direction suggests that E_z is the odd axis (Krantz, 1988).

In order to apply the odd-axis model to the study area, information is needed about the direction and magnitude of dip of the SAR structural features. A search of earthquake archives of the University of Nevada, Reno Seismological Laboratory listed 50 earthquakes in the study area, each with a focal mechanism solution. Figure 4 shows the locations of the epicenters and magnitudes of the earthquakes; twenty-one earthquakes occurred within the Excelsior-Coaldale section and 29 occurred within the Walker Lake section. Figure 5 is an index map for all the earthquake focal mechanisms in the study area. For the Excelsior-Coaldale section, all of the focal mechanisms show predominantly strike-slip movement, whereas in the Walker Lake section a number of the focal mechanisms indicate a dip-slip component, and the rest indicated strike-slip. Many of the focal mechanisms have a fault/auxiliary plane parallel or subparallel with one of the major SAR structural features. This allowed identification of the focal mechanism fault plane and an inferred slip vector. All strike-slip earthquakes in the Excelsior-Coaldale section were left-lateral, and all strike-slip earthquakes in the Walker Lake section were right-lateral. Many of the epicenters are located less than a kilometre from a SAR structural feature. The focal mechanisms for these earthquakes (Figure 2) were used to obtain information on dip magnitude, dip direction, and slip direction.

According to the odd-axis model (Krantz, 1988), the ratio of fault slip to fault spacing can be neglected for small ratio values, allowing use of the simplified equations for the strain ratios. Krantz (1988) has also determined that, for fault spacing ratios less than or equal to 0.1, the accuracy of the simplified strain ratio equations is greater than or equal to 96 percent.

Four traverses were taken across the SAR structural fea-

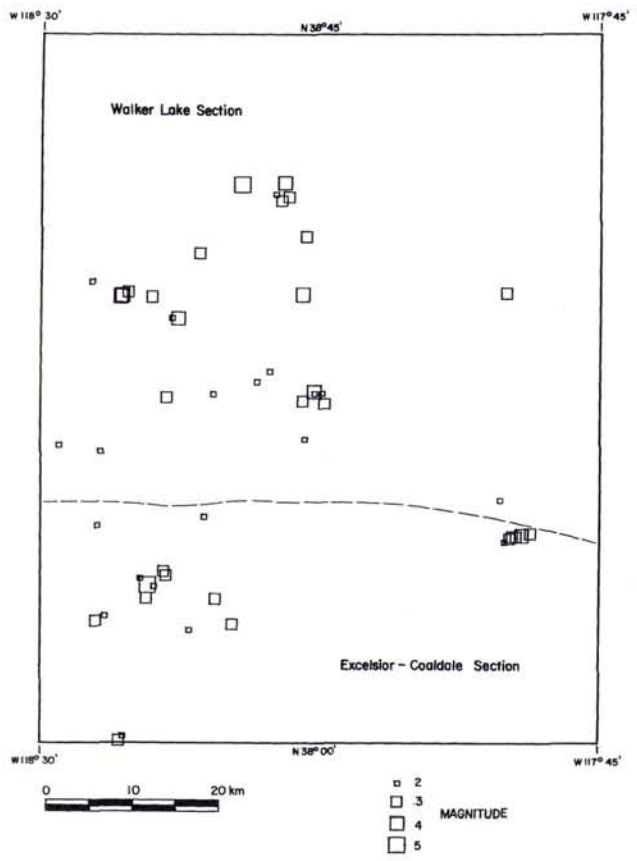

Figure 4. Location of earthquake epicenters with magnitude indicated.

tures, measuring the distance between each structural feature. The smallest average spacing is approximately 1.8 kilometres. For a fault-slip-to-fault-spacing ratio less than or equal to 0.1, fault slip must be less than or equal to 180 metres.

Watterson (1986) plotted maximum total displacement against fault length for 65 faults, thrusts, and groups of faults from a variety of geological environments (Figure 6). Displacements ranged from 0.4 metres to 40 kilometres and lengths from 150 metres to 630 kilometres, and he showed that a linear relationship exists between maximum total displacement and fault length. More than 90 percent of the SAR structural features in the study area are less than 10 kilometres in length. Based on Watterson's (1986) analysis, for an average linear strain of 10^{-3}, a fault 10 kilometres in length would have a total maximum displacement of less than 20 metres, and approximately 100 metres of total maximum displacement if the average linear strain was 10^{-2}. Although Watterson's (1986) model does not show data for strike-slip faults, fault slip for individual faults within the study area is surely less than 180 metres, and the simplified Equations 1, 2, and 3 can be used to calculate the strain ratios.

The odd-axis method of three-dimensional strain analysis was applied separately to the Walker Lake section and the Excelsior-Coaldale section. Using the stereonet construction of Krantz (1988), the poles to faults and the slip vectors from the focal mechanisms were plotted and aligned on great circles. Figure 7 is the stereonet odd-axis solution for three-dimensional strain for the Walker Lake section. The solid great circle that dips west on Figure 7 is an average of the three dashed great circles.

The poles to faults and the slip vectors for the Excelsior-Coaldale section were also plotted and aligned on great circles. The planes defined by the great circles were distributed across the stereonet in such a way that a unique odd-axis intersection could not be identified (Figure 8). This suggests that some of the assumptions of this approach are not correct for the Excelsior-Coaldale section. Although many of the SAR structural features in the Excelsior-Coaldale section are in Holocene sediments, many of the earthquakes may actually be occurring on Mesozoic (?) structures and may not provide nodal planes and slip vectors that are representative of Quaternary faults. The nodal planes and slip vectors from Mesozoic (?) structures would be different from those from Holocene sediments, and a scattered distribution of great circles on the stereonet would result. Table 1 lists the value for alpha; the strain ratios from Equations 1, 2, and 3; the plunge and azimuth of the principal strain ellipsoid axes; and the value for k for the Walker Lake section. Krantz (1988) defines k as the ratio of intermediate to minimum extension, where k can range from -0.5 (oblate) to 1 (prolate), with plane strain occurring where $k = 0$.

Because the three-dimensional strain from the odd-axis

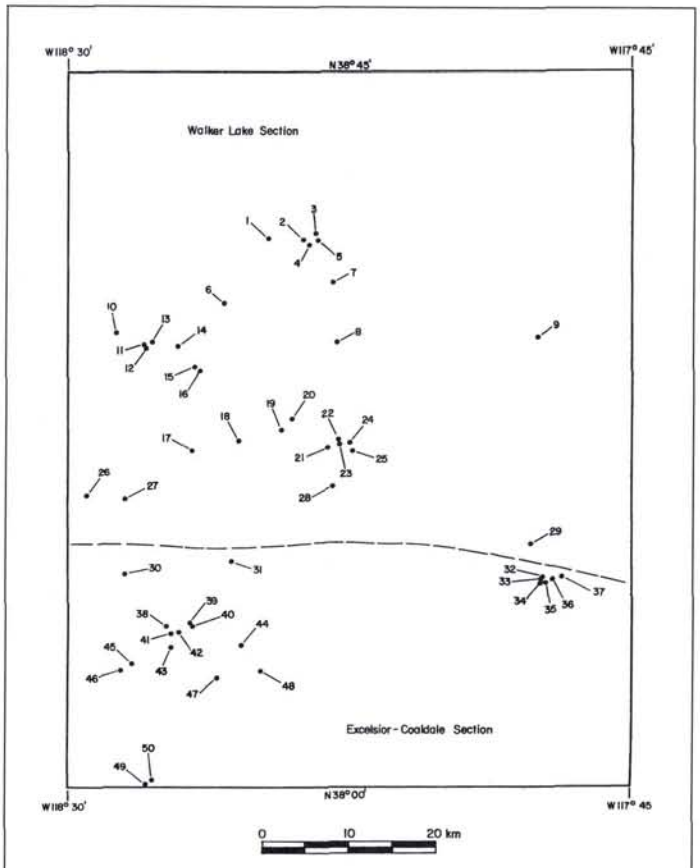

Figure 5. Index map for all the earthquake focal mechanisms.

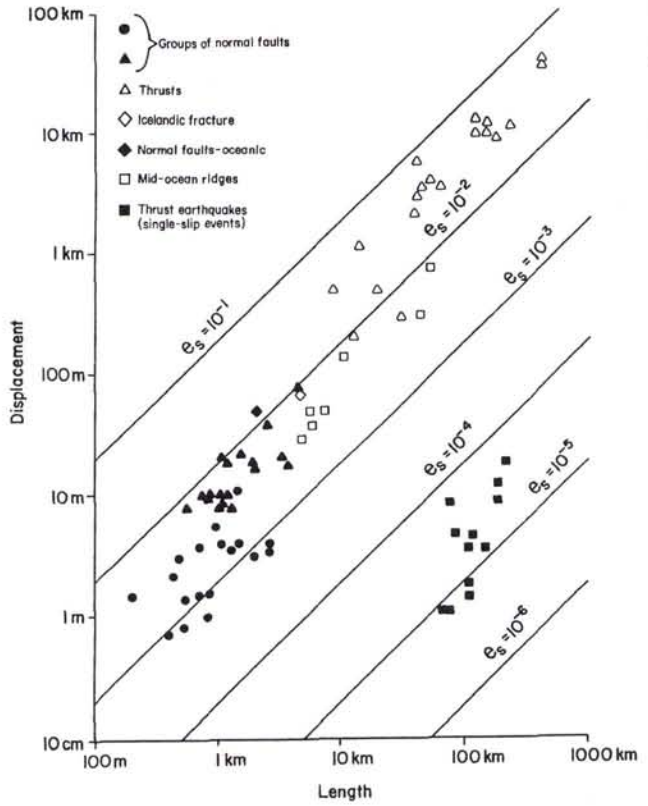

Figure 6. Total fault displacement plotted against fault length (modified from Watterson (1986)).

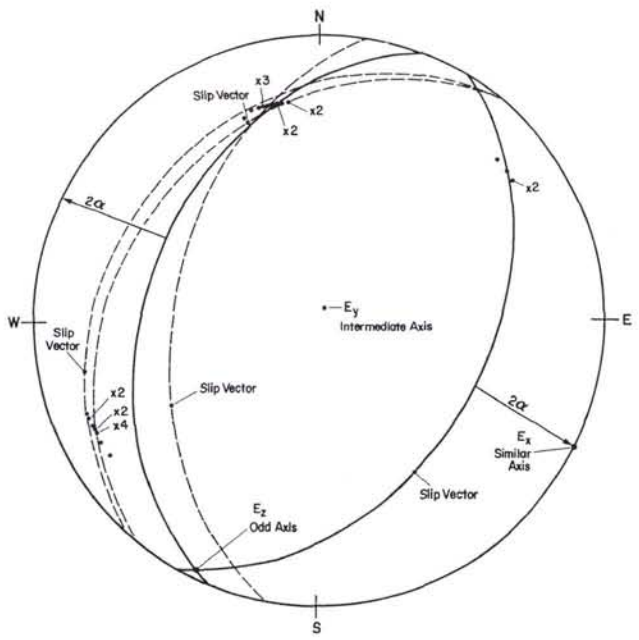

Figure 7. Stereonet odd-axis solution (Krantz, 1988) for the Walker Lake section of the Walker Lane.

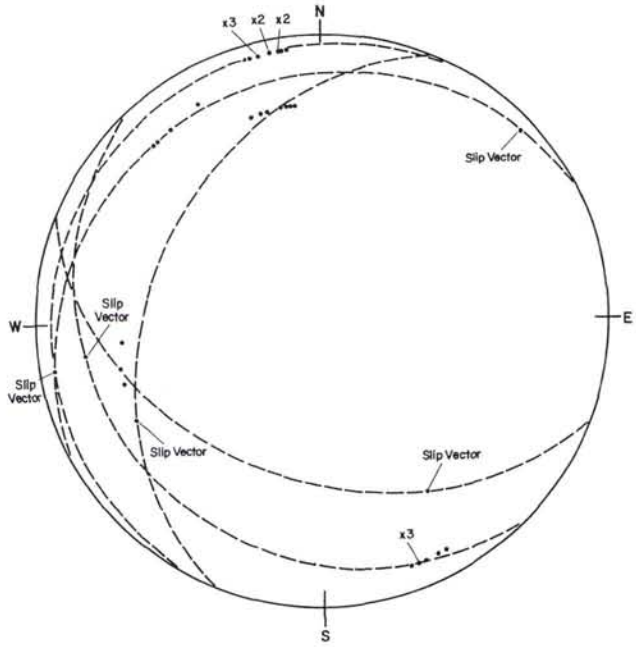

Figure 8. Poles to faults and slip vectors for the Excelsior-Coaldale section of the Walker Lane.

model (Krantz, 1988) is infinitesimal, the principal stresses, S_1, S_2, and S_3, can be determined directly ($E_z = S_1$, etc.). Table 2 lists the orientations of the principal stresses and the stress orientations calculated from stress inversion of earthquake focal mechanisms (U.R. Vetter, 1988, personal communication), and Figure 9 shows the plunge and azimuth of these stresses plotted on a stereonet. The stress tensor of Vetter was derived from earthquakes over a region that includes both the Walker Lake and Excelsior-Coaldale sections.

Discussions and Conclusions

The plunge of the three-dimensional strain analysis (Krantz, 1988) for the Walker Lake section agrees, rather closely, with the regional stress tensors of U.R. Vetter (1988, personal communication). This analysis used a subset of Vetter's data and this is, in part, a reason for the close agreement. However, the incorporation of SAR structural features into Krantz's (1988) three-dimensional strain analysis permitted a determination of the orientation of the infinitesimal strain el-

TABLE 1. ALPHA, STRAIN RATIOS, K, AND ORIENTATION OF THE PRINCIPAL STRAIN ELLIPSOID FOR THE WALKER LAKE SECTION

Walker Lake Section

alpha = 39.5°
$E_{int}/E_{sim} = \tan^2 \alpha = E_y/E_x = 0.68$
$E_{int}/E_{odd} = -\sin^2 \alpha = E_y/E_z = -0.40 = k$ (oblate)
$E_{sim}/E_{odd} = -\cos^2 \alpha = E_x/E_z = -0.60$

	Plunge	Azimuth
E_x	0°	116°
E_y	86°	26°
E_z	4°	206°

TABLE 2. ORIENTATIONS OF THE PRINCIPAL STRESSES AND THE STRESS ORIENTATIONS CALCULATED FROM STRESS INVERSION OF EARTHQUAKE FOCAL MECHANISMS

	Walker Lake Section	
	Plunge	Azimuth
S_1	4°	206°
S_2	86°	26°
S_3	0°	116°
	Stress Tensor	
	Plunge	Azimuth
S_1	5°	30°
S_2	85°	210°
S_3	0°	120°

lipsoid for the Walker Lake section. In addition, structural features mapped from imaging radar imagery can be used to identify the fault plane and auxiliary plane on earthquake focal mechanisms. In some cases, a SAR structural feature is coincident with an earthquake epicenter and is very likely the fault associated with the earthquake. The Walker Lake infinitesimal strain ellipsoid is flattened (oblate, $k = -0.40$) (Figure 10). The E_z axis of the strain ellipsoid is near-horizontal at an azimuth of 206°. With $k = -0.40$, E_x and E_y would be of approximately the same magnitude and the strain ellipsoid represents uniaxial flattening in a north-northeast direction. The E_y axis is nearly vertical and the E_x axis is horizontal and, because these two strain ellipsoid axes are approximately equal, extension is occurring in these directions. This is consistent with both focal mechanisms and existing field data, which indicate strike-slip, dip-slip, and oblique faulting. Because of inherited Mesozoic (?) structures in the Excelsior-Coaldale section, regional Walker Lane deformation is probably accommodated independently within the Walker Lake and Excelsior-Coaldale sections, and is not expressed as throughgoing strike-skip faults. Based on Stewart's (1985) work, major east-trending strike-slip faults were present before or at the beginning of the initiation of the Walker Lane and resulted in a rheological anisotropy between the Walker Lake and Excelsior-Coaldale sections. Inherited Mesozoic (?) structures, as well as rheological anisotropy, are probably the reason that a unique odd-axis stereonet solution cannot be determined for the Excelsior-Coaldale section.

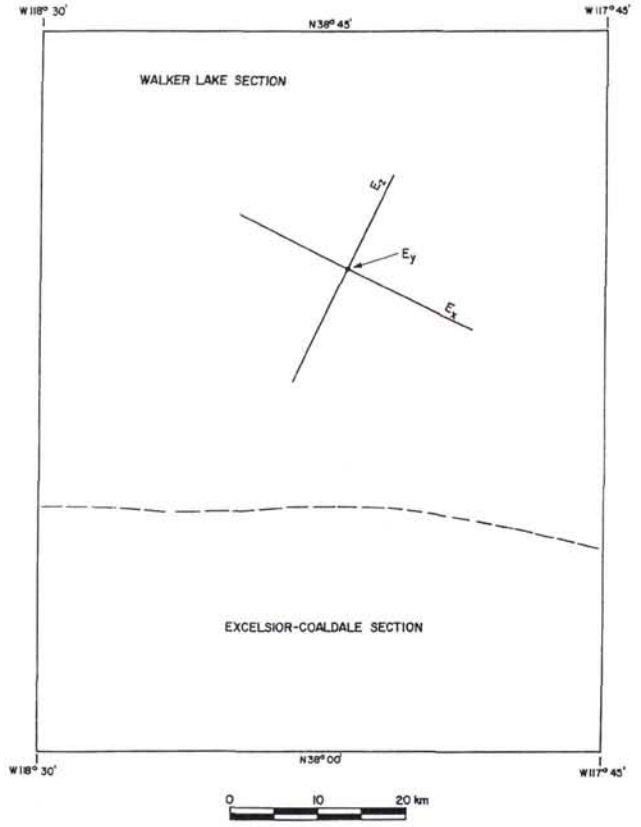

Figure 10. Orientation of the infinitesimal three-dimensional strain ellipsoid for the Walker Lake section of the Walker Lane.

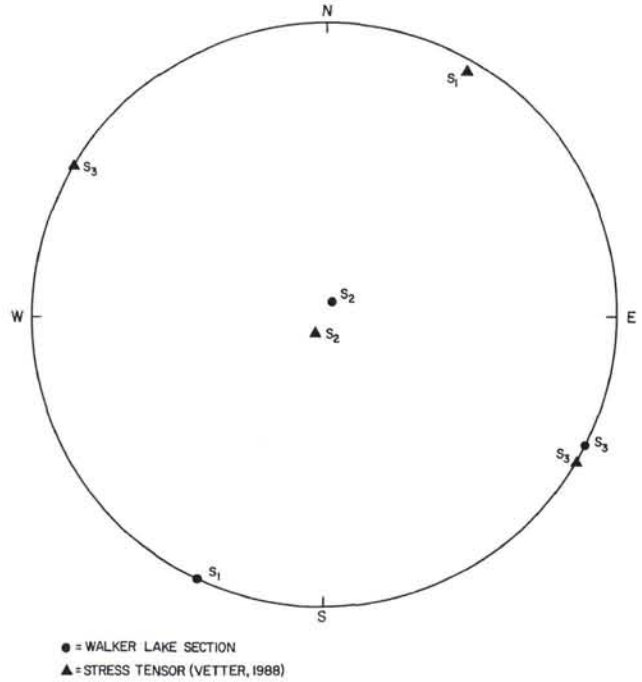

Figure 9. Orientations of the principal stresses from this study and the stress orientations calculated from stress inversion of the earthquake focal mechanisms (U.R. Vetter, 1988, personal communication).

Acknowledgments

Appreciation is extended to Spectro Scan, Inc., for assistance, especially William D. Bryant, Marilyn L. Sullivan, and Wayne D. Bock. The author also thanks Michael Ellis and Richard A. Schweickert for providing valuable input, and Laura L. Bryan and Kimberly Simmons for preparation assistance.

References

Albers, J. P., 1967. Belt of sigmoidal bending and right-lateral faulting in the western Great Basin, *Geol. Soc. American Bull.*, 78: 143-156.

Babaie, H. A., 1984. *Structure and Tectonics of the Golconda Allochthon*, Ph.D. Thesis, Northwestern University, Evanston, Illinois, 200 p.

Billingsley, P., and A. Locke, 1939. Structure of Ore Districts in the Continental Framework, *AIME Transactions*, 144:9-64.

Callaghan, E., and V.P. Gianella, 1935. The earthquake of January 30, 1934, at Excelsior Mountains, Nevada, *Seismol. Soc. America Bull.*, 25:161-168.

Carr, W.J., 1984. Timing and style tectonism and localization of volcanism in the Walker Lane Belt of southwestern Nevada, *Geol. Soc. Amer. Abstracts with Programs*, 16(6):464.

Ekren, E.B., and F.M. Byers, 1984. The Gabbs Valley Range — A well-exposed segment of the Walker Lane in west-central Nevada, *Western Geological Excursions, 1984 Annual Meeting of the Geological Society of America*, Volume 4.

Ekren, E.B., F.M. Byers, Jr., R.F. Hardyman, R.F. Marvin, and M.L. Silberman, 1980. *Stratigraphy, Preliminary Petrology, and some Structural Features of Tertiary Volcanic Rocks in the Gabbs Valley and Gillis Ranges, Mineral County, Nevada*, U. S. Geological Survey Bulletin 1464, 54 p.

Ferguson, H.G., and S.W. Muller, 1949. *Structural Geology of the Hawthorne and Tonopah Quadrangles, Nevada*, U.S. Geological Survey Professional Paper 216, 55 p.

Gianella, V.P., and E. Callaghan, 1934. The earthquake of December 20, 1932, at Cedar Mountain, Nevada, and its bearing on the genesis of Basin Range structure, *J. Geology*, 42:1-22.

Hardyman, R.G., 1978. *Volcanic Stratigraphy and Structural Geology of Gillis Canyon Quadrangle, Northern Gillis Range, Mineral County, Nevada*, unpubl. dissertation, University of Nevada-Reno, 377 p.

———, 1984. Strike-slip, normal and detachment faults in the northern Gillis Range, Walker Lane of west-central Nevada, *Western Geological Excursions* (Joseph Lintz, Jr., editor), Geol. Soc. America Ann. Meet., Mackay Sch. of Mines, Reno, Nevada, 4: 184-199.

Hardyman, R.G., E.B. Ekren, and F.M. Byers, Jr., 1975. Cenozoic strike-slip, normal and detachment faults in northern part of the Walker Lane, west central Nevada [abstract], *Geol. Soc. America Abstract with Programs*, 7(7):1100.

Krantz, R.W., 1988. Multiple fault sets and three-dimensional strain: theory and application, *Jour. Struct. Geology*, 10(3):225-237.

Molinari, M.P., 1984. Late Cenozoic structural geology of Stewart and Monte Cristo Valleys, Walker Lane of west central Nevada, *Western Geological Excursions* (Joseph Lintz, Jr., editor), Geol. Soc. America Ann. Meet., Mackay School of Mines, Reno, Nevada, 4:219-231.

Nielsen, R.L., 1965. Right-lateral strike-slip faulting in the Walker Lane, west-central Nevada, *Geol. Soc. Amer. Bull.*, 76:1301-1308.

Oldow, J.S., 1981. Kinematics of late Mesozoic thrusting, Pilot Mountains, Nevada, *J. Struct. Geol.*, 3:39-51.

———, 1984. Spatial variability in the structure of the Roberts Mountain allochthon, western Nevada, *Geol. Soc. Amer. Bull.*, 95:174-185.

Saleeby, J.B., with contributions by R.C. Speed, M.C. Blake, R.W. Allmendinger, P.B. Gans, R.W. Kistler, D.C. Ross, D.A. Stauber, M.L. Zoback, A. Griscom, D.S. McCulloch, A.H. Lachenbruch, R.B. Smith, and D.P. Hill (R.C. Speed, Coordinator) 1986. *Centennial Continent/Ocean Transect #10, C-2:Central California Offshore to Colorado Plateau*, Geol. Soc. America.

Speed, R.C., 1978. Paleogeographic and plate tectonic evolution of the early Mesozoic marine province of the western Great Basin, *Mesozoic Paleogeography of the Western United States* (D.G. Howell and K.A. McDougall, editors), Pacific Section, Soc. Econ. Paleontologists and Mineralogists, Pacific Coast Paleogeography Symposium 2, pp. 253-270.

Speed, R.C., and A.H. Cogbill, 1979. Candelaria and other left-lateral slip faults of the Candelaria region, Nevada, *Geol. Soc. America Bull.*, Part I, 90:149-163.

Speed, R.C., and R.W. Kistler, 1980. Cretaceous volcanism, Excelsior Mountains, Nevada, *Geol. Soc. America Bull.*, 91:392-398.

Stewart, J.H., 1980. *Geology of Nevada*, Nevada Bur. Mines and Geol. Spec. Pub. 4, 136 p.

———, 1985. East-trending dextral faults in the western Great Basin: An explanation for anomalous trends of pre-Cenozoic strata and Cenozoic faults, *Tectonics*, 4:547-564.

———, 1988. Tectonics of the Walker Lane Belt, Western Great Basin: Mesozoic and Cenozoic Deformation in a Zone of Shear, *Rubey*, 7:683-713.

Watterson, J., 1986. Fault dimensions, displacements and growth, *Pageoph*, 124(1/2):365-373.

Zoback, M.L., and S. Beanland, 1986. Temporal variations in stress magnitude and style of faulting along the Sierran frontal fault system, *Geol. Soc. America Abstr. with Programs*, 18:801.

(Received 2 August 1993; accepted 20 October 1993; revised 21 April 1994)

Marcus Borengasser
Marcus Borengasser received the B.S. and M.S. degrees in Geology from the University of Arkansas, and the Ph.D. in Geology from the University of Nevada, Reno. Dr. Borengasser is Vice President and Senior Scientist for Spectro Scan, Inc., and Adjunct Faculty in Physics and Space Sciences at Florida Tech.